

Synthesis and structures of tris(pentafluorophenyl)silylamines

V. V. Levin,^a A. D. Dilman,^{a*} A. A. Korlyukov,^{b*} P. A. Belyakov,^a M. I. Struchkova,^a
M. Yu. Antipin,^b and V. A. Tartakovsky^a

^aN. D. Zelinsky Institute of Organic Chemistry, Russian Academy of Sciences,
47 Leninsky prosp., 119991 Moscow, Russian Federation.
Fax: +7 (495) 135 5328. E-mail: dilman@ioc.ac.ru

^bA. N. Nesmeyanov Institute of Organoelement Compounds, Russian Academy of Sciences,
28 ul. Vavilova, 119991 Moscow, Russian Federation.
E-mail: alex@xrlab.ineos.ac.ru

Tris(pentafluorophenyl)silylamines were synthesized by silylation of amines and imines with (C₆F₅)₃SiCl or (C₆F₅)₃SiOTf in the presence of triethylamine. The crystal structures of the (C₆F₅)₃SiN(H)CH₂Ph and (C₆F₅)₃SiN(CH=CHMe)₂CH₂Ph compounds were studied by X-ray diffraction. The crystal packings were analyzed by quantum chemical calculations in terms of the density functional theory (PBE exchange-correlation functional).

Key words: amines, imines, silylation, organosilicon compounds, organofluorine compounds, X-ray diffraction analysis, quantum chemical calculations.

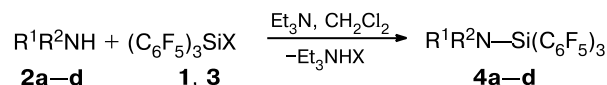
In the last few years, we have studied the chemistry of tris(pentafluorophenyl)silyl derivatives. Silanes, in which the (C₆F₅)₃Si fragment is bound to the oxygen^{1–4} or carbon^{5–7} atom, have received considerable attention. The key feature of these compounds is the high Lewis acidity of the silicon atom due to the presence of three electron-withdrawing pentafluorophenyl substituents. In particular, ROSi(C₆F₅)₃^{3,4} and MeSi(C₆F₅)₃^{6,7} proved to be convenient reagents in the transfer of the C₆F₅ group to iminium carbocations. In addition, the crystal structures of *O*- and *C*-tris(pentafluorophenyl)silyl derivatives are characterized by interesting features, in particular, by the presence of stacking interactions involving the C₆F₅ groups and very short Si—O and Si—C bonds.^{1–5}

In this connection, it was of interest to study analogous derivatives with the Si—N bond. Only one representative of tris(pentafluorophenyl)silylamines, Me₂NSi(C₆F₅)₃, was mentioned in the literature, but it was synthesized with the use of strongly basic anionic reagents by the reaction of lithium dimethylamide with (C₆F₅)₃SiCl (**1**) or by the reaction of pentafluorophenyllithium with Cl₃SiNMe₂.⁸

In the present study, we developed a simpler procedure for the synthesis of compounds containing the (C₆F₅)₃Si—N fragment based on the reaction of neutral nitrogen-containing precursors, such as amines and imines, with silylating reagents.

The silylation of primary and secondary amines with (C₆F₅)₃SiCl (**1**) in the presence of triethylamine in dichloromethane proceeds rapidly and smoothly (Scheme 1, Table 1, runs 1–3). This method was used

Scheme 1



X = Cl (**1**), OTf (**3**)

R¹ = H, R² = Bn (**a**); R¹ + R² = (CH₂)₄ (**b**); R¹ = H, R² = Ph (**c**);
R¹ = Me, R² = Ph (**d**)

for the preparation of the corresponding benzylamine, pyrrolidine, and aniline derivatives in high yields. However, under these conditions, *N*-methylaniline **2d** remained unconsumed in the reaction even upon prolonged storage of the reaction mixture (monitoring by ¹H NMR spectroscopy). The low reactivity of this substrate is, ap-

Table 1. Synthesis of tris(pentafluorophenyl)silylamines **4** by the reactions of amines or imines **2** with silanes (C₆F₅)₃SiX (X = Cl (**1**) or OTf (**3**))

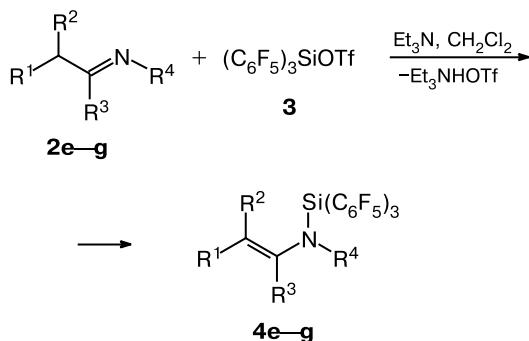
Run*	Substrate	Silane	T/°C	Product	Yield of compound 4 (%)
1	2a	1	–20→20	4a	88
2	2b	1	–20→20	4b	88
3	2c	1	–20→20	4c	92
4	2d	3	–20→20	4d	78
5	2e	3	0→20	4e	55
6	2f	3	20	4f	60
7	2g	3	0→20	4g	56

* The reaction time in runs 1–5 and 7 was 30 min; in run 6, 16 h.

parently, attributed to both the strong electronic effect of the benzene ring and the relative steric crowding of the nitrogen atom. To overcome this problem, we used the more powerful silylating reagent, *viz.*, tris(pentafluorophenyl)silyl triflate (**3**), in the presence of which *N*-methyl-aniline **2d** underwent rapid silylation (see Table 1, run 4).

Silyl chloride **1** also proved to be unsuitable for the silylation of imines. In this case, silyl triflate **3** is the reagent of choice (Scheme 2, see Table 1, runs 5–7). According to the ^1H NMR spectroscopic data, the silylation of imines **2e–g** proceeds almost quantitatively. However, the yields of silylated derivatives **4e–g** somewhat decreased after the isolation because of losses in the course of recrystallization.

Scheme 2



$\text{R}^1 = \text{R}^2 = \text{R}^4 = \text{Me}$, $\text{R}^3 = \text{H}$ (**e**); $\text{R}^1 = \text{R}^2 = \text{Me}$, $\text{R}^3 = \text{H}$, $\text{R}^4 = \text{Bn}$ (**f**); $\text{R}^1 + \text{R}^3 = (\text{CH}_2)_3$, $\text{R}^2 = \text{H}$, $\text{R}^4 = \text{Bn}$ (**g**)

Compounds **4a–g** were characterized by ^1H , ^{13}C , and ^{19}F NMR spectroscopy. Except for compound **4c**, these products are crystalline compounds. Since they are very sensitive to moisture, it is necessary to thoroughly remove traces of water when operating with these compounds. Compounds **4a–c** undergo rapid hydrolysis in air, due to which elemental analysis presents difficulty. For more stable derivatives **4d–f**, satisfactory analytical data were obtained.

The molecular and crystal structures of compounds **4a,f** were studied by X-ray diffraction (Figs 1 and 2, Tables 2 and 3). These structures are characterized by short Si–N bonds (1.6936(12) Å for **4a** and 1.7002(13) Å for **4f**), which are somewhat shorter than the analogous bonds in silylamines described earlier. For example, the Si–N bond length in triphenylsilylamines Ph_3SiNR_2 is 1.710 Å (in Ph_3SiNH_2 ,⁹ CCDC PECBUU) and 1.717 Å (in $\text{Ph}_3\text{SiNHSiPh}_3$,¹⁰ CCDC PDSILZ01), whereas the length of the shortest bond in compounds bearing three carbon-containing substituents at the silicon atom is 1.705 Å (in $\text{Bu}^t\text{N(H)Si(Me}_2\text{)C}\equiv\text{CSi(Me}_2\text{)N(H)Bu}^t$,¹¹ CCDC BUSIAC). Earlier, short Si–N bonds (<1.700 Å) have been observed only in derivatives containing the

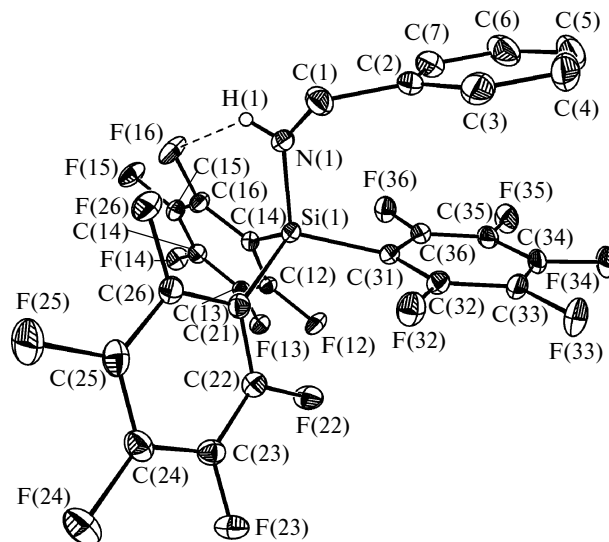


Fig. 1. Molecule **4a** represented by displacement ellipsoids at the 50% probability level. The H atoms, except for H(1), are omitted.

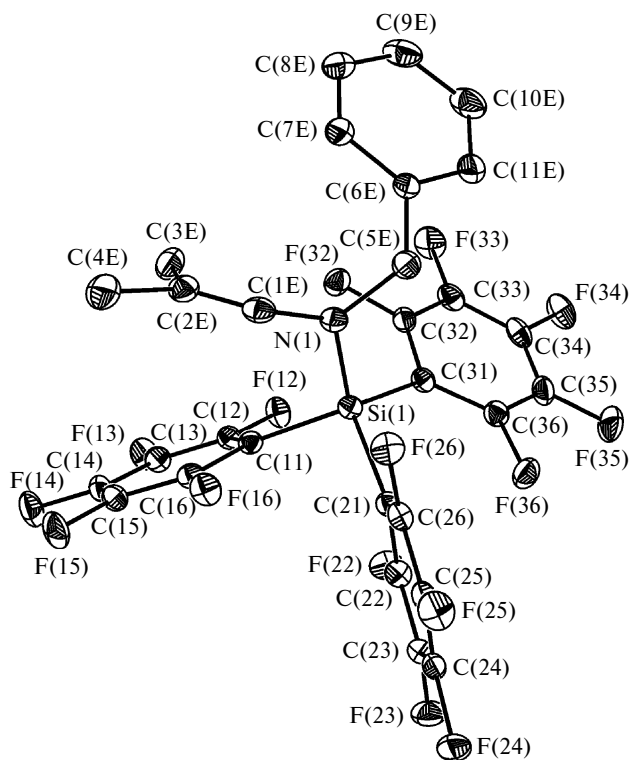


Fig. 2. Molecule **4f** represented by displacement ellipsoids at the 50% probability level. The H atoms are omitted.

fluoro or silyloxy substituents at the silicon atom ($r_{\text{Si–N}} = 1.694$ Å in $\text{Bu}^t_2\text{FSiN(H)CH}_2\text{CH}_2\text{N(H)SiFBu}^t_2$,¹² CCDC DABTAC; $r_{\text{Si–N}} = 1.685$ Å in $\text{ArF}_2\text{Si–NSi(OSiMe}_3\text{)Bu}^t_2$,¹³ CCDC FOKPAX; $r_{\text{Si–N}} = 1.696$ Å in $\text{Bu}^t_2(\text{R}_3\text{SiO})\text{SiNH}_2$,¹⁴ CCDC SASTUB; and $r_{\text{Si–N}} = 1.694$ Å in

Table 2. Selected bond lengths (*d*) and bond angles (ω) in the crystal structures and isolated molecules **4a,f**

Parameter	Crystal (experiment/calculations)		Isolated molecule (calculations)	
	4a	4f	4a	4f
Bond	<i>d</i> /Å			
Si(1)—N(1)	1.694(1)/1.709	1.700(1)/1.721	1.729	1.749
Si(1)—C(11)	1.888(1)/1.901	1.889(2)/1.899	1.913	1.916
Si(1)—C(21)	1.892(2)/1.908	1.893(2)/1.904	1.920	1.926
Si(1)—C(31)	1.886(1)/1.891	1.889(2)/1.897	1.903	1.918
N(1)—C(1)	1.469(2)/1.466	1.436(2)/1.426	—	2.386
N(1)—C(5E)	—	1.488(2)/1.486	—	2.384
C(1E)—C(2E)	—	1.328(2)/1.349	—	2.385
C(2)...C(31)	3.302(2)/3.270	—	3.515	—
C(2E)...C(11)	—	3.336(3)/3.358	—	3.607
N(1)...F(16)	2.811(2)/2.823	—	2.962	—
H(1)...F(16)	2.12/2.061	—	2.301	—
Angle	ω /deg			
N(1)—Si(1)—C(11)	112.91(6)/107.87	108.69(7)/108.56	108.3	110.7
N(1)—Si(1)—C(21)	113.99(6)/115.52	117.32(7)/117.78	115.6	117.2
N(1)—Si(1)—C(31)	107.04(6)/107.98	106.63(6)/106.73	105.2	104.7
N(1)—H(1)...F(16)	137.0/130.01	—	121.5	—
C(2)...C(7)—C(31)...C(36)	12.24/11.61	—	24.9	—
Si(1)—C(31)—C(31)...C(36)	9.98(8)/5.2	—	0.1	—

Table 3. Principal crystallographic parameters and the X-ray data collection and refinement statistics for compounds **4a,f**

Parameter	4a	4f
Molecular formula	C ₂₅ H ₈ F ₁₅ NSi	C ₂₉ H ₁₄ F ₁₅ NSi
Molecular weight	635.41	689.50
<i>T</i> /K	100	110(2)
<i>a</i> /Å	7.4933(3)	8.2391(4)
<i>b</i> /Å	16.1991(7)	16.7202(8)
<i>c</i> /Å	9.8958(4)	19.9490(9)
β /deg	103.325(1)	92.9170(10)
<i>V</i> /Å ³	1168.86(8)	2744.6(2)
<i>d</i> _{calc} /g cm ^{−3}	1.805	1.669
Space group	<i>P</i> 2 ₁	<i>P</i> 2 ₁ /c
<i>Z</i>	2	2
2 θ _{max} /deg	61	61
<i>F</i> (000)	628	1376
Scan mode	ω	ω
Number of measured reflections	14115	36625
Number of independent reflections (<i>R</i> _{int})	7028 (0.0223)	8382 (0.0429)
Number of observed reflections with <i>I</i> > 2 σ (<i>I</i>)	6546	6049
Number of variables	380	252
Absorption coefficient/cm ^{−1}	2.39	2.10
<i>R</i> ₁ (<i>I</i> > 2 σ (<i>I</i>))	0.0303	0.0405
<i>wR</i> ₂	0.0803	0.1033
Absolute structure parameter	0.52(8)	—
Residual electron density/e Å ^{−3} , ρ _{max} / ρ _{min}	0.34/−0.21	0.43/−0.28

$\text{MeCl}_2\text{SiN}(\text{Ar})\text{C}(\text{Ph})=\text{C}(\text{Ph})\text{N}(\text{Ar})\text{SiCl}_2\text{Me}$,¹⁵ CCDC RIJTAF).

Earlier, we have observed an analogous shortening of the Si—O and Si—C bonds in the tris(pentafluorophenyl)silyl derivatives $(\text{C}_6\text{F}_5)_3\text{SiOR}$ and $(\text{C}_6\text{F}_5)_3\text{SiCR}_3$.^{1–5} Apparently, this effect is a general property of the $(\text{C}_6\text{F}_5)_3\text{Si}$ fragment, which can be associated with the strong electron-withdrawing effect of the pentafluorophenyl substituents.

The nitrogen atom in molecules **4a,f** is characterized by noticeable pyramidalization. The sum of angles at the N(1) atom is 356.6 and 355.8°, respectively. This suggests that the electron density corresponding to the lone electron pair of the N(1) atom in both structures can additionally interact with the antibonding orbital of the Si(1)—C(21) bond, which is ~0.005 Å longer than the Si(1)—C(11) and Si(1)—C(31) bonds.

The recent analysis of the crystal and molecular structures of tris(pentafluorophenyl)silyl compounds has shown that the phenyl group and one of the pentafluorophenyl substituents in silanes $(\text{C}_6\text{F}_5)_3\text{SiCH}(\text{R})\text{Ph}$ (R = H or Me) are parallel to each other, the distance between the opposite carbon atoms being 3.1–3.3 Å, which is smaller than the sum of the van der Waals radii of these atoms (3.59 Å).⁵ In addition, a shortened intramolecular contact between the allyl group and the pentafluorophenyl substituent is observed in the structure of tris(pentafluorophenyl)allylsilane.⁵ This suggests that there is an intramolecular interaction between the C_i atom of the phenyl substituent or the CH group of the allyl substituent, which bear a high partial negative charge, and the C_j atom of the pentafluorophenyl group bearing a partial positive charge. This interaction is absent in the isolated molecules, because the above-described mutual arrangement of the substituents is absent in these molecules, as was demonstrated by the calculations.⁵ Apparently, this C...C interaction is rather weak. In molecules **4a,f**, the configuration of the substituents at the Si(1) atom is such that the interaction could occur between the phenyl (in **4a**) or 2-methylpropenyl (in **4f**) group of the amine fragment, on the one hand, and the C_6F_5 substituent, on the other hand. Actually, the angle between the planes of the phenyl and pentafluorophenyl groups in molecule **4a** is 12.24°, and the distance between the C(2) and C(31) atoms is 3.302(2) Å, which is 0.3 Å smaller than the sum of the van der Waals radii of these atoms.¹⁶ It should also be noted that the pentafluorophenyl group is bent toward the benzyl fragment, and the angle between the Si(1)—C(31) bond and the plane of the six-membered ring is 9.98(8)°. In molecule **4f**, there is a shortened contact between the C(2E) atom of the enamine fragment and the C(11) atom of the C_6F_5 group; the corresponding interatomic distance is 3.336(3) Å.

To study the character of interactions between the substituents in molecules **4a,f**, we performed quantum

chemical calculations for their crystal structures and isolated molecules. The atomic positions in the crystal structures and isolated molecules of compounds **4a,f** were optimized in terms of the density functional theory (the PBE exchange-correlation functional). The Si—C and Si—N bond lengths in the calculated crystal structures of **4a,f** are 0.01–0.02 Å longer than the experimental values. The quantum chemical calculations for the crystal structures reproduced the interatomic distances corresponding to the F...F and C—H...F intermolecular contacts with high accuracy (the differences between the calculated and experimental values are at most 0.04 and 0.1 Å, respectively). The C(2)...C(31) interatomic distance in the structure of **4a** is 0.03 Å shorter (the experimental and calculated bond lengths are 3.302(2) and 3.270 Å, respectively), whereas the C(2E)...C(11) distance in the structure of **4f** is, on the contrary, 0.01 Å longer compared to the corresponding distances determined by X-ray diffraction (3.336(3) and 3.358 Å, respectively).

In isolated molecules **4a,f**, the Si—N bond lengths are 0.03 Å larger than the corresponding experimental parameters in the crystal structures. The Si(1)—C(21) bond is, on the average, 0.02 Å longer than the Si(1)—C(11) and Si(1)—C(31) bonds. Hence, the anomeric effect of the lone pair of the N(1) atom in isolated molecules **4a,f** is overestimated compared to that in the crystal structures, where the corresponding differences are at most 0.01 Å. As opposed to the experimental and calculated crystal structures of **4a**, the parallel arrangement of the phenyl and pentafluorophenyl groups is not retained in the isolated molecule. The angle between the Si(1)—C(31) bond and the plane of the six-membered ring C(31)...C(36) decreases to 5.8°. At the same time, the C(2)...C(31) interatomic distance is 0.25 Å longer compared to that observed in the calculated crystal structure (3.270 and 3.515 Å, respectively). This suggests that the C(2)...C(31) interaction in isolated molecule **4a** is absent. In the free state, molecule **4a** adopts, apparently, the configuration providing minimal steric hindrance to the arrangement of the substituents at the silicon atom. This is also confirmed by a noticeable weakening of the N—H...F intramolecular bond; the H...F interatomic distance is 0.25 Å longer than that in the calculated crystal structure. An analogous situation is observed for molecule **4f**, in which the C(2E)...C(11) interatomic distance is 0.3 Å longer than that in the calculated crystal structure.

Unfortunately, the influence of weak intermolecular interactions on the molecular geometry of **4a,f** cannot be estimated in full measure based on the analysis of only the structural parameters. Hence, we performed the topological analysis of the calculated electron density distributions ($\rho(r)$) in the crystal structures in terms of Bader's topological theory of Atoms in Molecules (AIM).¹⁷ Earlier, we have applied this approach to investigations of a wide range of crystal structures.^{18,19} This approach allows

not only the examination of the nature of chemical bonds and weak interatomic distances but also the evaluation of their energy characteristics.

The qualitative analysis of the nature of interatomic interactions was performed with the use of deformation electron density maps. As can be seen from the deformation electron density map for molecule **4a** (Fig. 3, *a*), the electron density peak is located in the vicinity of the N(1) atom. This peak corresponds to the lone pair of the N(1) atom. The deformation electron density distribution

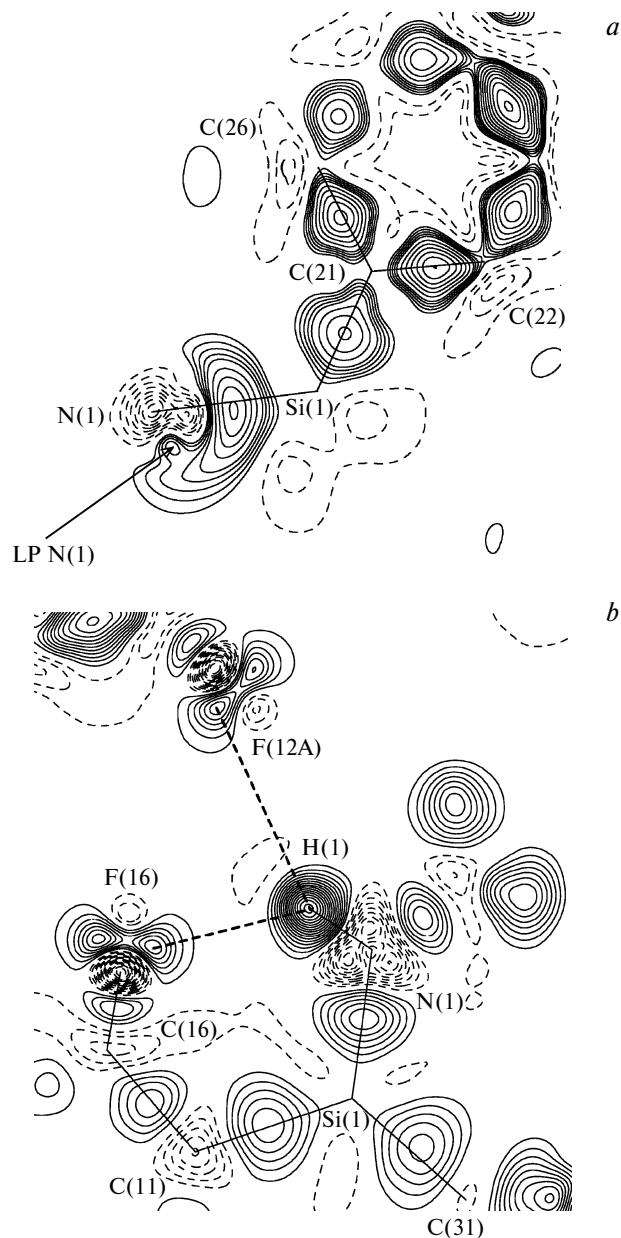


Fig. 3. Deformation electron density maps for compound **4a** in the N(1)Si(1)C(21) (*a*) and N(1)H(1)F(16) (*b*) planes contoured at $0.002 \text{ e } \text{\AA}^{-3}$ intervals. The negative values are indicated by dashed lines.

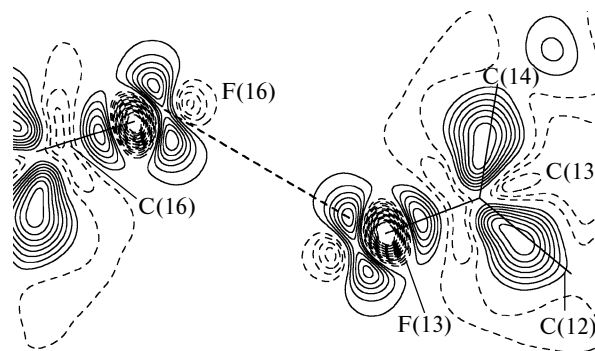


Fig. 4. Deformation electron density map for compound **4a** in the C(13)F(13)F(16) plane. The F(16) atom is generated by the symmetry operation $x + 1, y, z$. The map is contoured at $0.002 \text{ e } \text{\AA}^{-3}$ intervals. The negative values are indicated by dashed lines.

at the N(1) atom confirms the assumption that the lone pair of the N(1) atom interacts with the antibonding orbital of the Si(1)—C(21) bond. The H(1) atom at the nitrogen atom is involved in competitive N—H...F interactions (Fig. 3, *b*). In spite of the fact that the N—H...F intramolecular interaction is, apparently, stronger than the analogous intermolecular interaction, these interactions have the same nature. The shortened F...F contacts found in the crystal correspond to peak—hole interactions and are characterized by the orientation of the lone pair of one of the F atoms toward the region of electron density depletion of another F atom (Fig. 4).

The topological analysis of the $\rho(r)$ function in molecules **4a,f** revealed the presence of the critical points (3, -1) in the region of all expected chemical bonds and also in the region of shortened N—H...F, C—H...F, F...F, C...H, C...F, and C...C intra- and intermolecular contacts. The N—C and C—C bonds are characterized by the negative Laplacian of the electron density ($\nabla^2\rho(r)$) and the negative local energy density ($E^c(r)$) at the critical points (3, -1), *i.e.*, they are usual covalent bonds. At the critical points (3, -1) for the bonds involving the Si atom, $\nabla^2\rho(r)$ are positive, whereas $E^c(r)$ are negative, due to which these bonds can be assigned to an intermediate type of interatomic interactions. The N(1)—H(1)...F(16) intramolecular bond and the N—H...F, C—H...F, F...F, C...H, C...F, and C...C interatomic distances can be described as interactions between the closed shells ($\nabla^2\rho(r)$ and $E^c(r) < 0$ at the critical points (3, -1)).

The AIM theory allows the estimation of the energy of intermolecular contacts using correlation dependences.²⁰ The estimates obtained by this approach showed that the energy of the above-described weak intra- and intermolecular interactions varies from 0.5 to 1.2 kcal mol⁻¹ for C—H...F and N—H...F interactions, from 0.4 to 2.4 kcal mol⁻¹ for F...F, and from 0.7 to 1.1 kcal mol⁻¹ for C...C and C...H. The N(1)—H(1)...F(16) intramo-

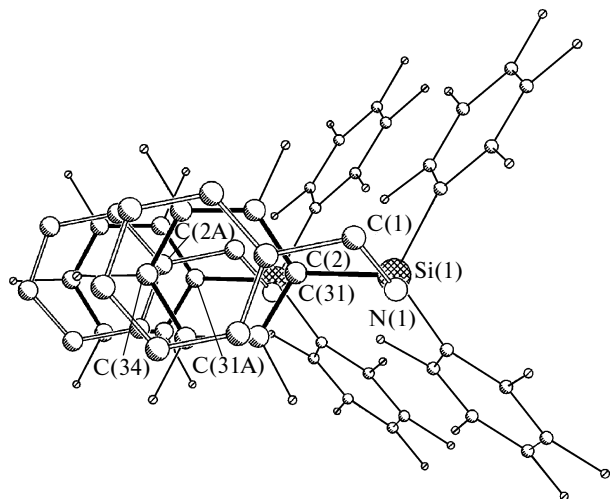


Fig. 5. Stacked arrangement of the molecules in the crystal structure of **4a**. The molecule A is generated from the reference molecule by the symmetry operation $x + 1, y, z$. The six-membered rings C(2)...C(7) are indicated by double lines.

molecular bond is slightly stronger than these interactions; its energy is $4.5 \text{ kcal mol}^{-1}$. One of advantages of this approach is that not only individual interactions but also the energy characteristics of different packing motifs can be estimated. For example, in the crystal structure of compound **4a**, the molecules are packed in stacks through stacking interactions between the phenyl and pentafluorophenyl groups (Fig. 5). The topological analysis revealed also the intramolecular interaction between these substituents. The intra- and intermolecular stacking interactions are almost equal in energy (0.80 and $1.07 \text{ kcal mol}^{-1}$, respectively). In addition, the stacking arrangement of the molecules is additionally stabilized by the intermolecular interaction between the C(36) atom and the methylene H(1AB) atom at the C(1) atom as well as by the F(22)...F(26) and F(23)...F(25) interactions, whose energies are 0.71 , 0.74 , and $0.68 \text{ kcal mol}^{-1}$, respectively. In the structure of **4f**, the critical point (3, -1) corresponding to the C(2E)...C(11) interaction was not found. Because of the structural features (steric hindrance), the intramolecular stacking interaction in this structure is absent. However, we found a weak intermolecular interaction of this type with the perfluorinated phenyl group C(31)...C(36). The energy of the latter interaction is low ($0.84 \text{ kcal mol}^{-1}$). The stacking interactions in the structures of **4a,f** are rather weak, and they are weaker than those observed for the monosubstituted benzene—perfluorinated benzene systems studied by quantum chemical methods at the high level of theory.²¹ Apparently, this is due to steric hindrance and also due to the fact that there are interactions in the crystal, which hinder the maximal overlap of the π systems.

The energy of the crystal lattice, which is generally approximately equal to the heat of sublimation, can be

determined²² by the summation of the energies of intermolecular contacts formed by molecules **4a,f**. The lattice energies calculated according to this approach are 17.82 and $10.94 \text{ kcal mol}^{-1}$, respectively. Apparently, the differences are associated with the stacking motif in the crystal packing of **4a**, resulting in an increase in the energy of intermolecular binding compared to that for compound **4f**, where this motif is absent. This conclusion is evidenced also by a comparison of the densities of compounds **4a** and **4f** (1.805 and 1.669 g cm^{-3} , respectively). The crystal packing of **4f**, in which the stacking arrangement of the molecules is absent, appeared to be less dense. The F...F interactions make the main contribution to the lattice energy. The number of these contacts is approximately the same in both structures. The stacking interactions and C—H...C contacts are responsible for an increase in the lattice energy in the structure of **4a**.

Experimental

The ^1H , ^{13}C , and ^{19}F NMR spectra were recorded on Bruker AM-300, Bruker WM-250, or Bruker AC-200 instruments in CDCl_3 , which was predistilled over CaH_2 and kept over molecular sieves 4 \AA . Dichloromethane was distilled over CaH_2 before use. Petroleum ether (b.p. $60\text{--}70^\circ\text{C}$) was distilled over LiAlH_4 and kept over molecular sieves 4 \AA . Commercially available amines **2a—d** (Acros) were purified by distillation. Imines **2e—g**²³ and silylating reagents **1**²⁴ and **3**² were prepared according to procedures described earlier.

Silylation of amines 2a—d. A mixture of silylating reagent **1** or **3** (3 mmol) and dichloromethane (6 mL) was cooled to -25°C . Then triethylamine (0.50 mL , 3.6 mmol) and amine **2** (3 mmol) were added. The reaction mixture was stirred for $\sim 1 \text{ min}$, the cooling bath was removed, and the mixture was kept for 30 min . The solvent was evaporated, and the residue was extracted with hot petroleum ether ($1 \times 6 \text{ mL}$, $2 \times 3 \text{ mL}$). The extracts were combined. Their further working-up depended on the properties of the products.

N-Benzyl-N-[tris(pentafluorophenyl)silyl]amine (4a). The solution was concentrated to $2/3$ of the initial volume. The product that precipitated was dissolved with heating, and the solution was slowly cooled to -20°C and kept at this temperature for $\sim 14 \text{ h}$. The cold solvent was decanted. The crystals were washed with petroleum ether and dried. Compound **4a** was obtained in a yield of 1.677 g , m.p. $92\text{--}93^\circ\text{C}$. ^1H NMR (300 MHz), δ : 2.33 (t, 1 H , NH, $J = 7.5 \text{ Hz}$); 4.11 (d, 3 H , CH_2 , $J = 7.5 \text{ Hz}$); $7.22\text{--}7.40$ (m, 5 H , Ph). ^{13}C NMR (75 MHz), δ : 46.1 ; 105.7 (tm, $J_{\text{C,F}} = 27.4 \text{ Hz}$); 126.9 ; 127.3 ; 128.6 ; 137.6 (dm, $J_{\text{C,F}} = 255.7 \text{ Hz}$); 140.9 ; 143.7 (dm, $J_{\text{C,F}} = 258.9 \text{ Hz}$); 149.2 (dm, $J = 245.2 \text{ Hz}$). ^{19}F NMR (188 MHz), δ : -160.8 (m, 6 F , F_m); -148.5 (tt, 3 F , F_p , $J = 19.7 \text{ Hz}$, $J = 5.2 \text{ Hz}$); -128.7 (d, 6 F , F_o , $J = 18.7 \text{ Hz}$).

1-[Tris(pentafluorophenyl)silyl]pyrrolidine (4b). The product slowly crystallized out during extraction. The combined extracts were heated until the crystals that precipitated were dissolved, and the resulting solution was slowly cooled to -20°C and kept at this temperature for $\sim 14 \text{ h}$. The cold solvent was decanted. The crystals were washed with petroleum ether and dried. Com-

pound **4b** was obtained in a yield of 1.582 g, m.p. 140–142 °C. ^1H NMR (300 MHz), δ : 1.75–1.87 (m, 4 H, $(\text{CH}_2)_2$); 3.00–3.13 (m, 4 H, $\text{N}(\text{CH}_2)_2$). ^{13}C NMR (50 MHz), δ : 26.8; 47.7; 106.3 (tm, $J_{\text{C,F}} = 28.4$ Hz); 137.6 (dm, $J_{\text{C,F}} = 254.1$ Hz); 143.6 (dt, $J_{\text{C,F}} = 258.0$ Hz, $J_{\text{C,F}} = 13.3$ Hz, $J_{\text{C,F}} = 6.2$ Hz); 149.4 (dm, $J = 246.3$ Hz). ^{19}F NMR (188 MHz), δ : –161.6 (m, 6 F, F_m); –149.4 (tt, 3 F, F_p , $J = 20.1$ Hz, $J = 4.5$ Hz); –129.3 (d, 6 F, F_o , $J = 18.7$ Hz).

***N*-[Tris(pentafluorophenyl)silyl]aniline (4c).** The solvent was removed. The residual oil was dried at 50 °C (~1 Torr). Compound **4c** was obtained in a yield of 1.715 g as a glassy substance. ^1H NMR (300 MHz), δ : 4.47 (s, NH); 6.75 (d, 2 H, Ph, $J = 7.7$ Hz); 6.91 (t, 1 H, Ph, $J = 7.4$ Hz); 7.17 (t, 2 H, Ph, $J = 7.7$ Hz). ^{13}C NMR (50 MHz), δ : 104.9 (tm, $J_{\text{C,F}} = 26.6$ Hz); 118.6; 121.4; 129.5; 137.7 (dm, $J_{\text{C,F}} = 256.2$ Hz); 142.6; 144.1 (dm, $J_{\text{C,F}} = 259.1$ Hz); 149.5 (dm, $J_{\text{C,F}} = 247.3$ Hz). ^{19}F NMR (188 MHz), δ : –160.5 (m, 6 F, F_m); –147.6 (tt, 3 F, F_p , $J = 20.1$ Hz, $J = 4.9$ Hz); –128.4 (d, 6 F, F_o , $J = 18.0$ Hz).

***N*-Methyl-*N*-[tris(pentafluorophenyl)silyl]aniline (4d).** The combined extracts were concentrated to one-half of the initial volume. The product that precipitated was dissolved with heating, and the solution was slowly cooled to –20 °C and kept at this temperature for ~14 h. The cold solvent was decanted. The crystals were washed with petroleum ether and dried. Compound **4d** was obtained in a yield of 1.487 g, m.p. 106–108 °C. Found (%): C, 47.35; H, 1.28; N, 2.20. $\text{C}_{25}\text{H}_8\text{F}_{15}\text{NSi}$ (635.40). Calculated (%): C, 47.26; H, 1.27; N, 2.20. ^1H NMR (250 MHz), δ : 3.02 (s, 3 H, Me); 6.97–7.10 (m, 3 H, Ph); 7.15–7.27 (m, 2 H, Ph). ^{13}C NMR (75 MHz), δ : 37.2; 106.0 (tm, $J_{\text{C,F}} = 27.9$ Hz); 121.9; 123.4; 129.1; 137.6 (dm, $J_{\text{C,F}} = 253.6$ Hz); 143.8 (dm, $J_{\text{C,F}} = 258.9$ Hz); 147.4; 149.3 (dm, $J = 245.7$ Hz). ^{19}F NMR (188 MHz), δ : –161.1 (m, 6 F, F_m); –148.3 (tt, 3 F, F_p , $J = 20.1$ Hz, $J = 4.9$ Hz); –128.3 (d, 6 F, F_o , $J = 18.7$ Hz).

Silylation of imines 2e–g. Triethylamine (0.50 mL, 3.6 mmol) and imine (3 mmol) were added to a suspension of silyl triflate (2.034 g, 3 mmol) in dichloromethane (6 mL) at 0 °C. In the case of imines **2e,g**, the reaction mixture was stirred at ~20 °C for 1 h. In the case of imine **2f**, the reaction mixture was heated until silyl triflate was dissolved and then kept at 20 °C for ~16 h. The solvent was evaporated, and the residue was extracted with boiling petroleum ether (1×6 mL, 2×3 mL). The combined extracts were concentrated to one-half of the initial volume. The product that precipitated was dissolved with heating, and the solution was slowly cooled to –20 °C and kept at this temperature for ~14 h. The cold solvent was decanted. The crystals were washed with petroleum ether and dried.

***N*-Methyl-*N*-(2-methylpropenyl)-*N*-[tris(pentafluorophenyl)silyl]amine (4e).** The yield was 1.012 g, m.p. 118–120 °C. Found (%): C, 45.07; H, 1.74; N, 2.21. $\text{C}_{23}\text{H}_{10}\text{F}_{15}\text{NSi}$ ($M = 613.39$). Calculated (%): C, 45.04; H, 1.64; N, 2.28. ^1H NMR (250 MHz), δ : 1.45 and 1.55 (both s, 3 H each, Me); 2.63 (s, 3 H, NMe); 5.65 (s, 1 H, CH). ^{13}C NMR (75 MHz), δ : 16.7; 21.8; 37.3; 106.0 (tm, $J_{\text{C,F}} = 27.4$ Hz); 127.2; 133.4; 137.5 (dm, $J_{\text{C,F}} = 254.1$ Hz); 143.6 (dm, $J = 258.4$ Hz); 149.4 (dm, $J_{\text{C,F}} = 246.8$ Hz). ^{19}F NMR (188 MHz), δ : –161.6 (m, 6 F, F_m); –148.9 (tt, 3 F, F_p , $J = 20.1$ Hz, $J = 4.9$ Hz); –128.1 (d, 6 F, F_o , $J = 19.4$ Hz).

***N*-Benzyl-*N*-(2-methylpropenyl)-*N*-[tris(pentafluorophenyl)silyl]amine (4f).** The yield was 1.241 g, m.p. 109–110 °C. Found (%): C, 50.67; H, 1.97; N, 2.03. $\text{C}_{29}\text{H}_{14}\text{F}_{15}\text{NSi}$ ($M = 689.49$). Calculated (%): C, 50.52; H, 2.05; N, 2.03.

^1H NMR (300 MHz), δ : 1.21 and 1.55 (both s, 3 H each, Me); 4.10 (s, 2 H, NCH_2); 5.68 (s, 1 H, CH); 6.97–7.06 (m, 3 H, Ph); 7.18–7.25 (m, 2 H, Ph). ^{13}C NMR (50 MHz), δ : 17.2; 22.0; 54.1 (quint, $J_{\text{C,F}} = 1.4$ Hz); 106.2 (tm, $J_{\text{C,F}} = 28.4$ Hz); 126.5 (q, $J_{\text{C,F}} = 1.4$ Hz); 127.4; 128.2; 128.3; 132.2; 137.6 (dm, $J = 254.8$ Hz); 138.3; 143.7 (dm, $J_{\text{C,F}} = 258.3$ Hz); 149.4 (dm, $J_{\text{C,F}} = 245.9$ Hz). ^{19}F NMR (188 MHz), δ : –161.3 (m, 6 F, F_m); –148.5 (tt, 3 F, F_p , $J = 20.1$ Hz, $J = 4.9$ Hz); –127.0 (d, 6 F, F_o , $J = 20.1$ Hz).

***N*-Benzyl-*N*-[tris(pentafluorophenyl)silyl]-*N*-(cyclopent-1-enyl)amine (4g).** The yield was 1.179 g, m.p. 95–96 °C. Found (%): C, 51.47; H, 1.99; N, 1.98. $\text{C}_{30}\text{H}_{14}\text{F}_{15}\text{NSi}$ ($M = 701.50$). Calculated (%): C, 51.36; H, 2.01; N, 2.00. ^1H NMR (300 MHz), δ : 1.77 (quint, 2 H, CH_2 , $J = 7.3$ Hz); 2.08–2.18 and 2.30–2.41 (both m, 2 H each, CH_2); 4.42 (s, 2 H, NCH_2); 4.88 (t, 1 H, CH, $J = 1.8$ Hz); 7.13–7.29 (m, 5 H, Ph). ^{13}C NMR (50 MHz), δ : 22.4; 30.0; 31.9; 50.8; 106.4 (tm, $J_{\text{C,F}} = 26.4$ Hz); 113.5; 126.5; 127.0; 128.3; 137.6 (dm, $J_{\text{C,F}} = 253.0$ Hz); 139.1; 143.6 (dm, $J_{\text{C,F}} = 258.7$ Hz); 146.1; 149.3 (dm, $J_{\text{C,F}} = 246.3$ Hz). ^{19}F NMR (188 MHz), δ : –161.1 (m, 6 F, F_m); –148.5 (tt, 3 F, F_p , $J = 20.1$ Hz, $J = 4.9$ Hz); –128.0 (d, 6 F, F_o , $J = 18.7$ Hz).

Quantum chemical calculations. All calculations for the crystal packings with full optimization of atomic positions were carried out with the use of the VASP 4.6.28 program,^{25–28} the PBE exchange-correlation potential,²⁹ and the plane wave basis set (the kinetic energy ≤ 400 eV). The core electrons were described with the PAW (projector augmented wave³⁰) pseudopotentials. For the topological analysis, the electron density function was calculated separately with the use of the hard PAW pseudopotentials and the dense fast-Fourier transform (FFT) grid. The topological analysis was carried out using the AIM program implemented in the ABINIT program package.³¹ The calculated $\rho(r)$ and $\nabla^2\rho(r)$ at the critical points (3, –1) were used for the calculations of the potential and kinetic energies in terms of the scheme proposed by Espinosa, Molins, and Lecomte.²⁰

Calculations for isolated molecules **4a,f** were carried out with the use of the PRIRODA program (the PBE functional and the TZ2P basis set).³²

The assignment of the optimized geometry of molecules **4a,f** to the potential minima was made based on the determination of the Hessian (second derivative) matrix.

X-ray diffraction study of crystals 4a,f. The crystallographic parameters and the principal X-ray diffraction data collection and refinement statistics are given in Table 2. The experiments were carried out on a Bruker APEX II diffractometer. The structures were solved by direct methods and refined by the full-matrix least-squares method based on F^2 with anisotropic displacement parameters for nonhydrogen atoms. The hydrogen atoms of the hydroxy groups were located in difference Fourier maps and refined isotropically. All calculations were performed with the use of the SHELXTL PLUS program package (version 5.10).³³

This study was financially supported by the Council on Grants of the President of the Russian Federation (Program for State Support of Leading Scientific Schools of the Russian Federation and Young Doctors, Grant MK-4483.2007.3) and the Presidium of the Russian Academy of Sciences (Program No. 8).

References

1. A. D. Dilman, P. A. Belyakov, A. A. Korlyukov, and V. A. Tartakovsky, *Tetrahedron Lett.*, 2004, **45**, 3741.
2. V. V. Levin, A. D. Dilman, P. A. Belyakov, A. A. Korlyukov, M. I. Struchkova, and V. A. Tartakovsky, *Eur. J. Org. Chem.*, 2004, 5141.
3. A. D. Dilman, P. A. Belyakov, A. A. Korlyukov, M. I. Struchkova, and V. A. Tartakovsky, *Org. Lett.*, 2005, **7**, 2913.
4. V. V. Levin, A. D. Dilman, P. A. Belyakov, A. A. Korlyukov, M. I. Struchkova, M. Y. Antipin, and V. A. Tartakovsky, *Synthesis*, 2006, 489.
5. A. D. Dilman, D. E. Arkhipov, A. A. Korlyukov, V. P. Ananikov, V. M. Danilenko, and V. A. Tartakovsky, *J. Organomet. Chem.*, 2005, **690**, 3680.
6. A. D. Dilman, D. E. Arkhipov, P. A. Belyakov, M. I. Struchkova, and V. A. Tartakovsky, *Izv. Akad. Nauk, Ser. Khim.*, 2006, 498 [*Russ. Chem. Bull., Int. Ed.*, 2006, **55**, 517].
7. A. D. Dilman, V. V. Levin, P. A. Belyakov, M. I. Struchkova, and V. A. Tartakovsky, *Synthesis*, 2006, 447.
8. M. F. Lappert and J. Lynch, *Chem. Commun.*, 1968, 750.
9. K. Ruhlandt-Senge, R. A. Bartlett, M. M. Olmstead, and P. P. Power, *Angew. Chem., Int. Ed.*, 1993, **32**, 425.
10. R. A. Bartlett and P. P. Power, *J. Am. Chem. Soc.*, 1987, **109**, 6509.
11. W. Clegg, U. Klingebiel, J. Neemann, G. M. Sheldrick, and N. Vater, *Acta Crystallogr., Sect. B*, 1981, **37**, 987.
12. B. Fredelake, C. Ebker, U. Klingebiel, M. Noltemeyer, and S. Schmatz, *J. Fluorine Chem.*, 2004, **125**, 1007.
13. S. Kliem, U. Klingebiel, M. Noltemeyer, and S. Schmatz, *J. Organomet. Chem.*, 2005, **690**, 1100.
14. D. Schmidt-Base and U. Klingebiel, *Z. Naturforsch., B: Chem. Sci.*, 1989, **44**, 395.
15. U. Herzog, G. Roewer, B. Ziemer, and B. Herrschaft, *J. Organomet. Chem.*, 1997, **533**, 73.
16. R. S. Rowland and R. Taylor, *Phys. Chem.*, 1996, **100**, 7384.
17. R. F. W. Bader, *Atoms in Molecules. A Quantum Theory*, Clarendon Press, Oxford, 1990.
18. A. A. Korlyukov, S. A. Pogozhikh, Yu. A. Ovchinnikov, K. A. Lyssenko, M. Yu. Antipin, A. G. Shipov, O. A. Zamyshlyayeva, E. P. Kramarova, V. V. Negrebetky, I. P. Yakovlev, and Yu. I. Baukov, *J. Organomet. Chem.*, 2006, **691**, 3962.
19. K. A. Lyssenko, A. A. Korlyukov, D. G. Golovanov, S. Yu. Ketkov, and M. Yu. Antipin, *J. Phys. Chem. A*, 2006, **110**, 6545.
20. E. Espinosa, E. Molins, and C. Lecomte, *Chem. Phys. Lett.*, 1998, **285**, 170.
21. B. W. Gung and J. C. Amicangelo, *J. Org. Chem.*, 2006, **71**, 9261.
22. L. L. Shipman, A. W. Burgess, and H. A. Scheraga, *J. Phys. Chem.*, 1976, **80**, 52.
23. G. Bianchetti, P. D. Croce, D. Pocar, and A. Vigevari, *Gazz. Chim. Ital.*, 1967, **97**, 289.
24. H.-J. Frohn, A. Lewin, and V. V. Bardin, *J. Organomet. Chem.*, 1998, **568**, 233.
25. G. Kresse and J. Hafner, *Phys. Rev. B*, 1993, **47**, RC558.
26. G. Kresse, Ph. D. Thesis, Technische Universität Wien, Wien, 1993.
27. G. Kresse and J. Furthmüller, *Comput. Mat. Sci.*, 1996, **6**, 15.
28. G. Kresse and J. Furthmüller, *Phys. Rev. B*, 1996, **54**, 11169.
29. J. P. Perdew, S. Burke, and M. Ernzerhopf, *Phys. Rev. Lett.*, 1996, **77**, 3865.
30. G. Kresse and D. Joubert, *Phys. Rev. B*, 1999, **59**, 1758.
31. X. Gonze, J.-M. Beuken, R. Caracas, F. Detraux, M. Fuchs, G.-M. Rignanese, L. Sindic, M. Verstraete, G. Zerah, F. Jollet, M. Torrent, A. Roy, M. Mikami, Ph. Ghosez, J.-Y. Raty, and D. C. Allan, *Comput. Mat. Sci.*, 2002, **25**, 478.
32. D. N. Laikov, *Chem. Phys. Lett.*, 1997, **281**, 151.
33. G. M. Sheldrick, *SHELXTL-97, V5.10*, Bruker AXS Inc., Madison, WI-53719, USA, 1997.

Received January 9, 2007;
in revised form April 9, 2007